Authors' response

RC1 (Anonymous referee)

1. *Obviously, the authors have made an effort to maximize the efficiency of the hetero-nuclear decoupling by expanding the original 16 step supercycle to 64 steps and by applying a very high RF field strength of 24 kHz, covering the bandwidth in excess of 60 kHz (4000 ppm at 0.33 T, 14 MHz 1H). Since the CH proton chemical shift range at this field strength is less than 42 Hz (3 ppm) perhaps a simple CW decoupling would have been more efficient. It would also offer means of altering the size of the effective hetero-nuclear coupling.*

Response: The homogeneity of 0.33 T region of 2F NMR spectrometer is about 10 ppm, which is much worse than that typical for high-field NMR instruments (for example, the homogeneity of 14.1 T main field is about 0.05 ppm). To make sure that the ^{1}H-^{13}C interactions are suppressed in the entire sample volume the bandwidth of composite decoupling was increased. The broadband decoupling method used here required only 0.5 W RF power at 14 MHz; thus, it does not impose any problems such as sample heating.

Changes made: clarifying statements are added.

2. *Introduction: when describing slow and fast passage through the LAC the authors should indicate the time scale that is used to define what is fast and what is slow. I would guess it is the J-coupling (H-C, C-C, multiplet structure, etc.) that defines the desired time scale. Please clarify.*

Response: We have added clarifying sentences, explicitly introducing the adiabaticity parameter.

3. *Page 3, section B, lines 2 and 3: the proton resonance frequency is provided for the 14.1 T field, but not for the more unusual 0.33 T field. Please correct.*

Response: Done

4. *Page 3, section B, paragraph 2: the authors use RE-BURP refocusing pulse for inversion - nothing wrong with that, except the reader might be curious about the selection of the pulse shape, e.g. why not use an inversion pulse, such as I-BURP or G3?*

Response: The use of RE-BURP has no strict prerequisites. However, RE-BURP is a general-rotation 180° pulse which is less sensitive to the initial nuclear magnetization state than I-BURP (https://doi.org/10.1016/0022-2364(91)90034-Q) and has narrower excitation profile in comparison with G3.

Changes made: clarifying statement is added.

5. *Page 3, line 112: "WALTZ-64 supercycle" should be "WALTZ decoupling with MLEV-64 supercycle". A reference to MLEV-64 should be given along with that for the WALTZ decoupling.*

Response: Done

6. *Caption to Figure 2: the RF field strength for the 0.56 W decoupling at B(HF) should be given.*

Response: Done

7. *Page 11, lines 346-348, the last statement before the section V (Conclusions): please indicate that this statement is for abundant (or labelled) spins only.*

Response: We have added a clarifying statement just before the conclusions.

RC2 (Stephan Appelt)

2a: *A small confusion arises due to Figure 1, where the ^{13}C spectrum from L-leucine measured at 100.62 MHz is shown. Later in Figure 5 the ^{13}C spectra is presented at 150.9 MHz. The reader will ask why the ^{13}C NMR spectrum has not been measured at 150,9 MHz?*

Response: The ^{13}C spectrum of L-leucine was measured both at 100.62 MHz and 150.9 MHz, the resolution of the 100.62 MHz spectrum is better than one of 150.9 MHz.

Changes made: Figure 1 was corrected to present 150.9 MHz 13C spectrum of L-leucine

2b: *In section B in line 99 an unprecise statement is made "First, a non-equilibrium state is generated at B_HF by applying a selective pulse". Please specify here that a selective 180◦ pulse is applied to Cˆ(delta2), leading to a non-equilibrium state, i.e into a population inversion (refer here to Figure 2).*

Response: Done

2c: *There is an error in the signs in Equation (1), either all signs in the Zeeman terms (- om1 I1z- om2 I2z- om3 Sz) are negative or all are positive, but mixed signs cannot be true. Furthermore Equation (1) and (10) are inconsistent with Equation (2), where all signs before I1z and Sz are negative*

Response: Sign error in eqn. (1) is now corrected. We believe that there is no inconsistency between eqn. (10) and eqn. (2).

2d: *The exact form of om1, om2 and om3 should be stated in line 139, i.e. om1 = gam_C(1+delt2) B_HF, om2 = gam_C (1+deltgam) B_HF and om3 = gam_H B_HF.*

Response: we introduce omega's explicitly and explain all parameters.

2e: *The experimental results in Figures 5B and 6B are in good agreement with the theoretical expectation only in the first 10 ms. Especially in Figure 6B the experimental data does not show the oscillating features as suggested by the theory. An explanation for this deviation would be very helpful.*

Response: In the original version this issue, non-ideal agreement between theory and experiment, has been addressed. We attribute it to two factors: (i) relaxation effects, not taken into account in the simulation, (ii) lack of the precise knowledge of the B(t) profile. No changes are made in the text, since we do not have any further comments on this.

3. Technical corrections, typing errors and references:

Response: Changed as requested.

Comments from Nino Wili

1) The situation where heteronuclear couplings "quench" the effect of a strong homonuclear coupling appears similar to the origin of the "spin diffusion barrier" in EPR/DNP. In the latter, a difference in hyperfine couplings between protons and an unpaired electron inhibits the efficient polarization transfer between these protons, even if there is a strong homonuclear dipolar coupling between them. Hyperfine decoupling reduces this effect. Some readers with a different background might find it helpful if this similarity is pointed out (if you agree it is there).

Response: we agree that there is a similarity of the two phenomena. This analogy is mentioned in the conclusions and a review paper on spin diffusion by Ramanathan is cited.

2) I find it a bit awkward to use "surprising" in a title.

Response: we decided to make the title a bit "catchy".

3) Eq (1): it seems there should be a minus sign before ω1. Or is it intentionally left out?

Response: corrected, this was a typo.

4) You give the homonuclear J-couplings in table 1. Could you also give the 1H-13C couplings of the protons that couple to these carbons? Or did I miss them?

Response: corrected, direct J(CH) coupling values are also listed in Table 1.

5) Related to 4) Would you be willing to share your simulation code? I would be interested to look at the influence of different couplings strengths and field-cycling speeds

Response: we can share the code on request.

Surprising absence of strong homonuclear coupling at low magnetic field explored by two-field NMR spectroscopy

Ivan V. Zhukov,[1,2] Alexey S. Kiryutin,[1,2] Ziqing Wang,[3] Milan Zachrdla,[3] Alexandra V. Yurkovskaya,[1,2] Konstantin L. Ivanov,[1,2,*] Fabien Ferrage[3*]

[1] *International Tomography Center, Siberian Branch of the Russian Academy of Sciences, Novosibirsk, 630090, Russia*

[2] *Novosibirsk State University, Novosibirsk, 630090, Russia*

[3] *Laboratoire des Biomolécules, LBM, Département de chimie, École normale supérieure, PSL University, Sorbonne Université, CNRS, 75005 Paris, France*

* Konstantin L. Ivanov, ivanov@tomo.nsc.ru

* Fabien Ferrage, fabien.ferrage@ens.psl.eu

Abstract

Strong coupling of nuclear spins, which is achieved when their scalar coupling $2\pi J$ is greater than or comparable to the difference $\Delta\omega$ in their Larmor precession frequencies in an external magnetic field, gives rise to efficient coherent longitudinal polarization transfer. The strong-coupling regime can be achieved when the external magnetic field is sufficiently low, as $\Delta\omega$ is reduced proportional to the field strength. In the present work, however, we demonstrate that in heteronuclear spin systems these simple arguments may not hold, since heteronuclear spin-spin interactions alter the $\Delta\omega$ value. The experimental method that we use is two-field NMR (Nuclear Magnetic Resonance), exploiting sample shuttling between a high field, at which NMR spectra are acquired, and low field, where strong couplings are expected, at which NMR pulses can be applied to affect the spin dynamics. By using this technique, we generate zero-quantum spin coherences by means of non-adiabatic passage through a level anti-crossing and study their evolution at low field. Such zero-quantum coherences mediate the polarization transfer under strong coupling conditions. Experiments performed with an ^{13}C labelled amino acid clearly show that the coherent polarization transfer at low field is pronounced in the ^{13}C-spin subsystem under proton decoupling. However, in the absence of proton decoupling, polarization transfer by coherent processes is dramatically reduced, demonstrating that heteronuclear spin-spin interactions suppress the strong coupling regime even when the external field is low. A theoretical model is presented, which can simulate the reported experimental results.

I. Introduction

The topological and conformational information provided by scalar couplings lies at the foundation of the analytical power of NMR spectroscopy (Ernst et al., 1987; Keeler, 2005; Levitt, 2008; Cavanagh, 2007). The strong coupling case is encountered when scalar coupling constants are not negligible with respect to the difference of resonance frequency between the coupled spins (Keeler, 2005). Understanding strong scalar couplings and their spectral signature was essential when NMR was introduced for chemical analysis, which was typically performed at magnetic fields considered today as low (Bodenhausen et al., 1977; Pfändler and Bodenhausen, 1987). Modern high-field NMR is widely based on the exploitation of weak scalar couplings, so that strong scalar couplings have remained a nuisance, in particular in aromatic spin systems (Vallurupalli et al., 2007; Foroozandeh et al., 2014). Recently, the development and availability of benchtop NMR spectrometers operating at low or moderate magnetic fields (Grootveld et al., 2019), has revived the interest in the understanding of strong scalar couplings in conventional NMR.

Contrarily to conventional NMR, NMR at near-zero or ultralow magnetic fields (ZULF-NMR), explores the benefits of NMR in the strong scalar-coupling regime. At such magnetic fields, typically smaller than 1 μT, scalar coupling interactions dominate all Zeeman interaction and dictate the eigenstates of spin systems and transition energies obtained in spectra (Ledbetter et al., 2011; Tayler et al., 2017; Blanchard and Budker, 2016). However, for homonuclear couplings, the transition between the weak- and strong-coupling regimes occurs in a range of magnetic fields, where the Zeeman interaction is still dominant (Ivanov et al., 2006; Ivanov et al., 2008; Ivanov et al., 2014; Appelt et al., 2010; Türschmann et al., 2014). This transition between weak and strong couplings can be investigated by varying the magnetic field applied to the sample on a high-field magnet, which is usually performed by moving the sample through the stray field with a shuttle system (Roberts and Redfield, 2004a, b; Redfield, 2012; Wagner et al., 1999; Bryant and Korb, 2005; Goddard et al., 2007; Chou et al., 2016; Chou et al., 2017; Charlier et al., 2013; Cousin et al., 2016a; Cousin et al., 2016b; Zhukov et al., 2018; Kiryutin et al., 2016). These studies have highlighted the effects of level anti-crossings (LACs) (Miesel et al., 2006; Ivanov et al., 2014). When the passage through a LAC is slow, the transition is adiabatic and the population of eigenstates is smoothly converted to the new eigenstates. When the transition is fast, coherences can be generated between the new eigenstates and time-oscillations of the population of high-field eigenstates can be observed (Pravdivtsev et al., 2013; Kiryutin et al., 2013). This phenomenon has been observed on a variety of homonuclear spin systems. Heteronuclear scalar couplings have been shown to alter LACs in homonuclear spin systems (Korchak et al., 2012); yet, the properties of such heteronuclear couplings on LACs are not fully understood, in particular, in spin systems with extensive networks of homo- and heteronuclear scalar couplings. As usual, non-adiabatic variation, which gives rise to excitation of coherences, means that the adiabatic eigenstates of the spin system change with time fast as compared to the rate of internal evolution of the system. Specifically, for each pair of adiabatic states, $|i\rangle$ and $|j\rangle$, the parameter

$$\xi_{ij} = \frac{\langle j \left| \frac{d}{dt} \right| i \rangle}{\omega_{ij}}$$

Is much greater than 1 (here ω_{ij} is the energy difference between the states, measured in angular frequency units). When $\xi_{ij} \ll 1$, switching is adiabatic and populations follows the time-dependent eigenstates.

Here, we investigate the effect of heteronuclear scalar couplings on LACs in a spin system typical of biomolecular NMR, a uniformly carbon-13 labeled amino acid (leucine), which combines extensive networks of homo- and heteronuclear scalar couplings. Essentially, we exploit the ability to apply composite pulse decoupling on our two-field NMR spectrometer (Cousin et al., 2016a) to switch on and off heteronuclear scalar couplings at low magnetic field. We demonstrate that heteronuclear scalar couplings alter LACs by sustaining the weak-coupling regime in a carbon-13 homonuclear spin system.

80 Composite pulse decoupling at low magnetic field restores the strong scalar coupling regime in the
81 carbon-13 nuclei of the isopropyl group of leucine at 0.33 T. Our results identify how heteronuclear
82 couplings alter homonuclear couplings at low magnetic fields, which could be exploited in low-field NMR
83 methodology and may be considered in further developments of total correlation spectroscopy (TOCSY)
84 (Braunschweiler and Ernst, 1983) mixing sequences in high-field NMR.

II. Methods

A. Sample preparation

87 Experiments have been performed using the following sample: 76 mM 99% enriched $^{13}C,^{15}N$ labeled L-
88 leucine (Leu) in 90% H_2O 10% D_2O solution. $^{13}C,^{15}N$ enriched L-leucine were purchased from Sigma-Aldrich
89 and used as it stands. ^{13}C-NMR spectrum of the labelled Leu molecule is shown in **Figure 1**. We also show
90 separately the signals of the individual carbon nuclei. Broadband proton decoupling was used to simplify
91 the spectrum. Here, we will focus on a three-spin system, formed by the C^γ and two C^δ nuclei of the
92 isopropyl moiety. We will study polarization transfer in this subsystem upon fast switch of the external
93 magnetic field obtained by a transfer of the sample though the stray field of a high-field NMR magnet.
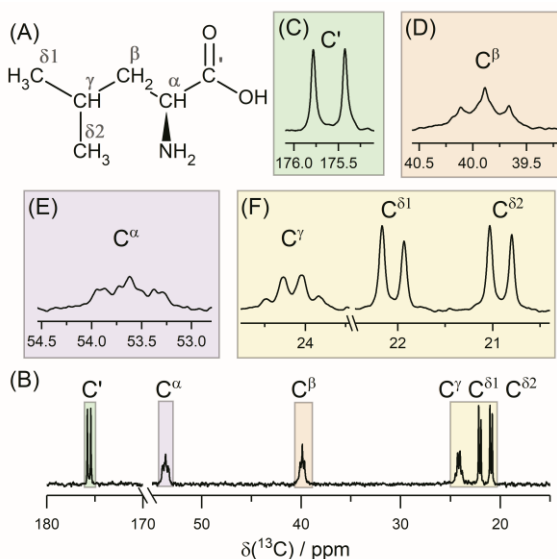
95 **Figure 1**. Structure of ^{13}C, ^{15}N L-leucine (A) and 150.9 MHz ^{13}C-NMR spectrum (B) under broadband ^1H decoupling.
96 Signal of each carbon nuclei is also shown separately (C)-(E). The multiplet structure in the spectrum is due to ^{13}C-
97 ^{13}C and ^{13}C-^{15}N scalar interactions.

B. Field-cycling NMR experiments

99 NMR experiments were performed on a two-field NMR spectrometer (Cousin et al., 2016a) with fast
100 sample shuttling (Charlier et al., 2013). The high field $B_{HF} = 14.1$ T is the detection field of a 600 MHz
101 NMR spectrometer while the low field is $B_{LF} = 0.33$ T corresponding to 14 MHz ^1H NMR frequency. The
102 magnetic field in the low-field centre is sufficiently homogeneous (inhomogeneities of the order of 10
103 ppm) so that radiofrequency (RF) pulses can be applied by using a triple-resonance NMR probe, as
104 described previously (Cousin et al., 2016a).

105 Field-cycling NMR experiments were run according to the pulse sequences depicted in **Figure 2**. First, a
106 non-equilibrium state is generated at B_{HF} by applying a selective π pulse to the $C^{\delta 2}$ nucleus (shaped RE-
107 BURP pulse (Geen and Freeman, 1991), the pulse duration was 46.4 ms, the peak RF-field amplitude was
108 adjusted to cover *ca*. 100 Hz bandwidth around the center of $C^{\delta 2}$ signal). RE-BURP shaped pulse was used
109 since it is less sensitive to the initial nuclear magnetization state than I-BURP (Geen and Freeman, 1991)
110 and has narrow excitation profile. To improve the selectivity of the pulse, simultaneous proton decoupling
111 was used, which reduces multiplet overlap in the carbon-13 NMR spectrum. Following this preparation,

112   the sample was shuttled from the high-field center to the low-field center $B_{HF} \rightarrow B_{LF}$ with a duration
113    $t_1 = 110$ ms. The field jump is fast enough to be non-adiabatic and it is aimed to excite a spin coherence.
114   Subsequently, the coherence evolves at B_{LF} during a variable time period τ. The shuttle transfer back to
115   the high-field center leads to a second field jump $B_{LF} \rightarrow B_{HF}$ with a duration $t_2 = 95$ ms. This second non-
116   adiabatic field jump to B_{HF} converts the coherence into a population difference. Detection is performed
117   after a $\pi/2$ pulse on the carbon-13 channel in the presence of proton decoupling. We perform two types
118   of experiments, in which the carbon spin coherence (zero-quantum coherence, ZQC) evolves at B_{LF} in the
119   absence (see **Figure 2A**) and in the presence (see **Figure 2B**) of proton composite-pulse decoupling.
120   Decoupling at B_{LF} has been performed using composite pulse decoupling pulse with the WALTZ
121   decoupling with MLEV-64 supercycle (Shaka et al., 1983; Levitt et al., 1982) at low field on the proton RF-
122   channel (operating at 14 MHz corresponding to the proton NMR frequency at 0.33 T). Composite pulse
123   decoupling is used because of the rather high inhomogeneity of the B_{LF} field, which is of the order of 10
124   ppm: under such conditions continuous-wave decoupling would require higher power, potentially giving
125   rise to sample heating. The τ-dependence of polarization is expected to be oscillatory, due to the coherent
126   polarization exchange within the expectedly strongly coupled system of the C^γ and two C^δ carbon-13
127   nuclei.
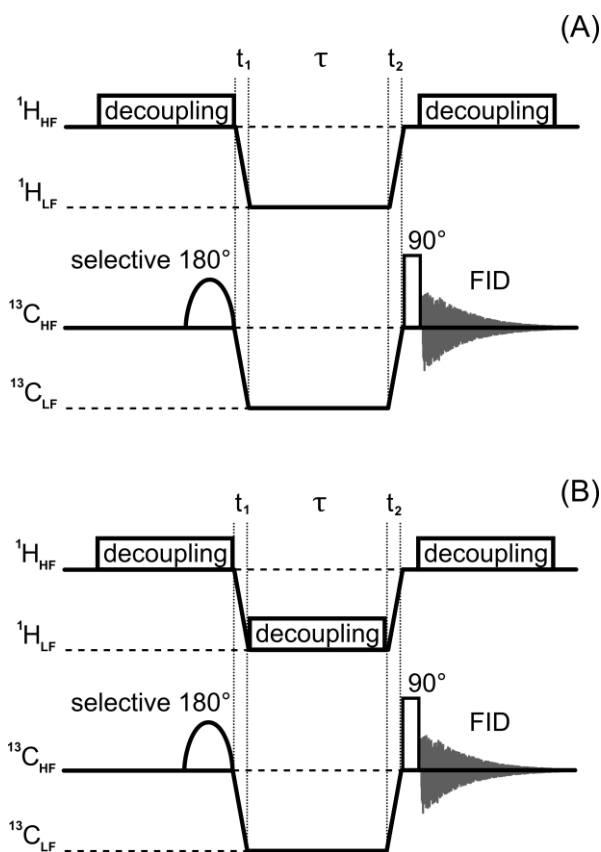
128
129   **Figure 2**. Experimental protocols of field-cycling NMR experiments without ^{1}H decoupling at the low field (A) and
130   with 24 kHz WALTZ-64 ^{1}H decoupling at the low field (B). Details of the experiments: 0.56 W (10 KHz) WALTZ-64
131   composite pulse decoupling on the proton channel was applied at B_{HF} during 100 ms prior to a selective 180-degree
132   pulse, in order to enhance ^{13}C polarization by the nuclear Overhauser effect. The sample shuttle times, t_1 and t_2,
133   were 80 ms and 120 ms, respectively. Selective inversion was performed with a ReBurp pulse (Geen and Freeman,
134   1991) with a duration of 46.4 ms at the $C^{\delta 2}$ resonant frequency covering *ca.* 100 Hz bandwidth. The delay τ at low
135   field was incremented with a 5 ms step. After sample transfer to high field, a hard 90-degree pulse generated [13]C
136   transverse magnetization; FID acquisition was done during 1.56 s under 2.7 kHz WALTZ-64 proton decoupling.

137   ## III. Theory

138   ### A. Polarization transfer in a 3-spin system

139 In this subsection, we provide a theoretical description of the field-cycling NMR experiments. First, we
140 present the analytical treatment of polarization transfer among two nuclei of the same kind, here spin I_1
141 and spin I_2 (*e.g.* two carbon-13 nuclei), in the presence of a third spin S, which can be a heteronucleus
142 (*e.g.* here a proton). This is the minimal system allowing us to detail the effect of a heteronucleus on
143 polarization transfer among strongly coupled spins. We assume that spins I_1 and I_2 are in strong coupling
144 conditions, meaning that the difference, $\Delta\omega$, in their Zeeman interaction frequencies with the external
145 field is smaller than or comparable to the scalar-coupling constant, $2\pi J_{12}$, between them. When the
146 strong coupling regime is achieved, the zero-quantum part of the scalar coupling, given by the operator
147 $\{\hat{I}_{1+}\hat{I}_{2-} + \hat{I}_{1-}\hat{I}_{2+}\}$, becomes active, giving rise to flips and flops of spins I_1 and I_2. The couplings to the
148 third spin S, J_{13} and J_{23}, are assumed to be unequal (otherwise coupling to the proton gives rise to an
149 identical shift of the NMR frequencies of spins 1 and 2 and does not modify the eigenstates of this
150 subsystem). The Hamiltonian of the spin system can be written as follows (in $\hbar$ units):

$$\hat{\mathcal{H}}_{CCH} = -\omega_1\hat{I}_{1z} - \omega_2\hat{I}_{2z} - \omega_3\hat{S}_z + 2\pi J_{12}(\hat{\mathbf{I}}_1 \cdot \hat{\mathbf{I}}_2) + 2\pi J_{13}\hat{I}_{1z}\hat{S}_z + 2\pi J_{23}\hat{I}_{2z}\hat{S}_z \qquad (1)$$

151 Here $\hat{\mathbf{I}}_1$, $\hat{\mathbf{I}}_2$ and $\hat{\mathbf{S}}$ are the spin operators; $\omega_1 = \gamma_I(1 + \delta_1)B$, $\omega_2 = \gamma_I(1 + \delta_2)B$ and $\omega_3 = \gamma_S(1 + \delta_1)B$
152 stand for the NMR frequencies of the corresponding nuclei (with $\gamma_{I,S}$ being the corresponding
153 gyromagnetic ratios, δ_i being the chemical shifts and B being the magnetic field strength). We assume
154 that the heteronucleus S is coupled weakly to I spins due to the large difference in their NMR frequencies,
155 i.e., $|\omega_1 - \omega_3|, |\omega_2 - \omega_3| \gg |\omega_1 - \omega_2|, 2\pi J_{13}, 2\pi J_{23}$, and keep only the secular part of the heteronuclear
156 coupling Hamiltonian.

157 In the present case, the nuclear magnetic number, m_S, of spin S is a "good quantum number", which is
158 conserved because $\hat{S}_z$ commutes with the Hamiltonian. For this reason, it is possible to find the solution
159 for the spin dynamics of spins I_1 and I_2 for two separate cases, which corresponds to the two different
160 values of m_S being $+\frac{1}{2}$ and $-\frac{1}{2}$, i.e., spin S is in the "spin-up" $|\alpha\rangle$ state or "spin-down" $|\beta\rangle$ state. In each
161 case, the Hamiltonian of the carbon subsystem is as follows:

$$\hat{\mathcal{H}}_{CC} = -\{\omega_1 - 2\pi J_{13}S_z\}\hat{I}_{1z} - \{\omega_2 - 2\pi J_{23}S_z\}\hat{I}_{2z} + 2\pi J_{12}(\hat{\mathbf{I}}_1 \cdot \hat{\mathbf{I}}_2) \qquad (2)$$

162 Hence, in the Hamiltonian given by eq. (1) we replace the $\hat{S}_z$ operator by the m_S value, which is $\pm\frac{1}{2}$. Hence,
163 the $\Delta\omega$ value is modified and it depends on the m_S value:

$$\Delta\omega_\pm = \{\omega_1 - \omega_2\} \mp \pi\{J_{13} - J_{23}\} = \Delta\omega \mp \pi \cdot \Delta J \qquad (3)$$

164 The eigenstates of the subsystem of spin 1 and spin 2 are

$$|1\rangle = |\alpha\alpha\rangle, \quad |2\rangle_\pm = \cos\theta_\pm |\alpha\beta\rangle + \sin\theta_\pm |\beta\alpha\rangle \qquad (4)$$
$$|3\rangle_\pm = -\sin\theta_\pm |\alpha\beta\rangle + \cos\theta_\pm |\beta\alpha\rangle, \quad |4\rangle = |\beta\beta\rangle$$

165 Here the "mixing angle" is given by the values of $\Delta\omega_\pm$ and J_{12}: $\tan 2\theta_\pm = 2\pi J_{12}/\Delta\omega_\pm$. When $\Delta\omega_\pm$
166 approaches zero, the mixing angle goes to $\frac{\pi}{4}$ meaning that the eigenstates become singlet and triplet
167 states: the spins are strongly coupled. When $\Delta\omega_\pm$ is much greater than the coupling, the eigenstates are
168 obviously the Zeeman states.

169 Even in this simple system, it is clear that the condition $|\omega_1 - \omega_2| \ll 2\pi J_{12}$ is not sufficient to guarantee
170 strong coupling of the two carbons. Indeed, when $2\pi\Delta J$ is greater than $\Delta\omega$ and $2\pi J_{12}$ the carbon spins
171 become weakly coupled in the two sub-ensembles, corresponding to $m_S = \pm\frac{1}{2}$.

172 How do heteronuclear couplings affect polarization transfer in the carbon system? We assume that at $t =$
173 0 one of the spins has polarization $\langle I_{1z}\rangle = P_0$ and the other spin is not polarized, $\langle I_{2z}\rangle = 0$. Hereafter, it
174 is convenient to use normalization $P_0 = 1$. The state of the spin system is then given by the density
175 operator

$$\sigma_0 = \hat{I}_{1z} \tag{5}$$

176 As shown previously (Ivanov et al., 2006), in the two-spin system of I_1 and I_2, in the absence of coupling
177 to any other spin, the polarization evolves with time as follows:

$$\langle I_{1z}\rangle(t) = 1 - \sin^2\theta\,\frac{1-\cos[\omega_{ZQC}t]}{2}, \quad \langle I_{2z}\rangle(t) = \sin^2\theta\,\frac{1-\cos[\omega_{ZQC}t]}{2} \tag{6}$$

178 where $\tan 2\theta = 2\pi J_{12}/\Delta\omega$ and the oscillation frequency $\omega_{ZQC} = \sqrt{\Delta\omega^2 + (2\pi J_{12})^2}$ is the frequency of
179 the ZQC between the eigenstates $|2\rangle$ and $|3\rangle$. Hence, coherent exchange of polarization is taking place.
180 As $\Delta\omega$ becomes smaller the frequency of the oscillations decreases, but the amplitude increases: at $\Delta\omega \to$
181 0 we obtain $\omega_{ZQC} = 2\pi|J_{12}|$ and complete exchange is possible when $t = 1/(2J_{12})$.
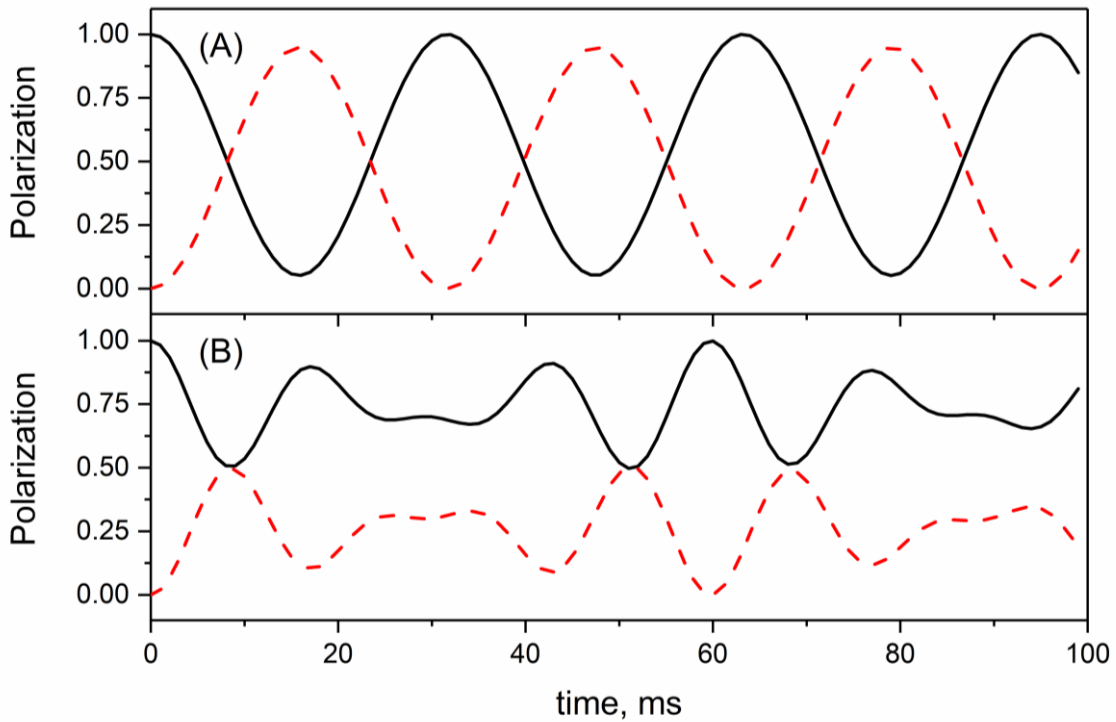
182
183 **Figure 3**. Polarization transfer among two strongly coupled nuclei (A) in the absence and (B) in the presence (bottom)
184 of a heteronucleus. Here, we present the time dependence of $\langle I_{1z}\rangle$ (black solid lines) and $\langle I_{2z}\rangle$ (red dashed lines),
185 normalized to the initial value of $\langle I_{1z}\rangle$. The density operator at time $t = 0$ is $\sigma_0 = \hat{I}_{1z}$. Parameters of the simulation
186 were $\Delta\omega/2\pi = 10$ Hz, $J_{12} = 30$ Hz, and (a) $\Delta J = 0$ Hz and (b) $\Delta J = 100$ Hz.

187 In the presence of scalar couplings to the third spin S, here a proton (I_1 and I_2 are carbon-13 nuclei), the
188 expressions should be modified: the evolution should be calculated for each specific spin state of the
189 proton, $|\alpha\rangle$ and $|\beta\rangle$, and sum of the two curves should be taken. We obtain at the following expression:

$$\langle I_{1z}\rangle(t) = 1 - \sin^2\theta_+\,\frac{1-\cos[\omega_{ZQC}^+ t]}{4} - \sin^2\theta_-\,\frac{1-\cos[\omega_{ZQC}^- t]}{4} \tag{7}$$

$$\langle I_{2z}\rangle(t) = \sin^2\theta_+\,\frac{1-\cos[\omega_{ZQC}^+ t]}{4} + \sin^2\theta_-\,\frac{1-\cos[\omega_{ZQC}^- t]}{4}$$

190 where the evolution frequencies are equal to $\omega_{ZQC}^\pm = \sqrt{\Delta\omega_\pm^2 + (2\pi J_{12})^2}$.

191 The time dependence of the expectation value for the longitudinal polarizations of spins I_1 and I_2 is
192 presented in **Figure 3** in the presence and the absence of scalar couplings to a heteronucleus. In the
193 absence of heteronuclear coupling the two strongly coupled spins (the strong coupling condition is
194 fulfilled since $2\pi J_{12} > \Delta\omega$) almost completely exchange polarizations. The polarization transfer is of a

coherent nature and the frequency of the oscillations is given by the scalar-coupling constant J_{12}. In the presence of different heteronuclear scalar couplings to the third spin S, the time-evolution changes considerably. The two spins are no longer in the regime of strong coupling, since $\left|\Delta\omega_{\pm}\right| > 2\pi J_{12}$. The efficiency of polarization transfer is reduced and complete exchange of polarization is no longer possible. The time dependence also becomes more complex: instead of a single frequency ω_{ZQC} found in the previous case, here two frequencies appear: ω_{ZQC}^{+} and ω_{ZQC}^{-}. Hence, when couplings to heteronuclei are present, the condition $\Delta\omega \sim 2\pi J_{12}$ does not guarantee that the homonuclei are in the strong-coupling regime.
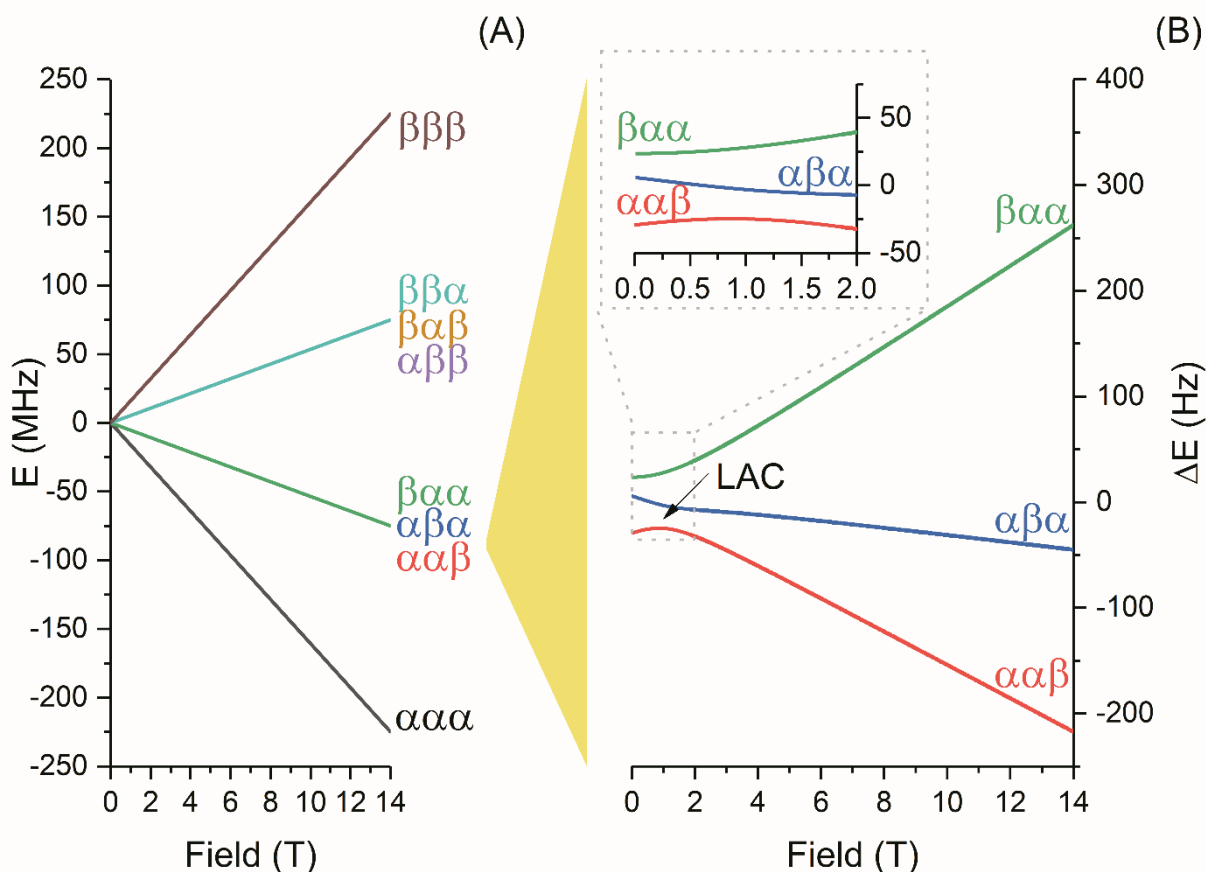
Figure 4. (A) Energy levels of the $\{C^{\gamma}, C^{\delta 1}, C^{\delta 2}\}$ spin system at variable magnetic field strength in the absence of scalar coupling with protons. Levels are assigned at high field, where the spin system is weakly coupled. (B) energy levels, corresponding to the $\alpha\alpha\beta$ and $\alpha\beta\alpha$ states at high field, have a LAC at 1.1 T, which is responsible for generation of the zero quantum coherences. To visualize the energy levels better, in the right panels we have subtracted the large Zeeman energy from the actual energy and show the energy difference. The calculation is done using parameters listed in **Table 1** and neglecting carbon-proton couplings.

These results show that the interaction with a heteronucleus clearly alters polarization transfer in strongly coupled networks. Consequently, we expect strong effects of heteronuclear interactions on polarization transfers in systems with several heteronuclei. Notably, we anticipate that polarization transfer among strongly coupled carbon spins will be dramatically different in the presence of proton decoupling, which effectively removes proton-carbon spin-spin interactions.

B. Spin dynamics simulations

In addition to this simple model, we carried out numerical simulations in a realistic multi-spin system: the isopropyl group of carbon-13 labeled leucine. This spin system contains three carbon-13 nuclei I_1, I_2, and I_3: the C^{γ} carbon-13 and the two C^{δ} carbon-13 nuclei. In addition, the spin system includes seven protons

219 S_i: each C^δ nucleus is coupled to the three protons of the methyl group, and the C^γ carbon-13 nucleus is
220 coupled to one proton. We model the effects of fast field variation and coherent spin dynamics at low
221 field. We consider two cases, namely, polarization transfer in the presence and in the absence of proton
222 decoupling.

223 The simulation method is as follows. The band-selective inversion pulse on spin I_3 generates the initial
224 density operator for the three-spin I system:

$$\sigma_0 = \sigma(t = 0) = \hat{I}_{1z} + \hat{I}_{2z} - \hat{I}_{3z} \tag{8}$$

225 Hence, we generate a population difference for the states $|\alpha\alpha\beta\rangle$, $|\alpha\beta\alpha\rangle$ and $|\beta\alpha\alpha\rangle$: the first state is
226 overpopulated, while the other two states are underpopulated. The three-spin system under study, C^γ,
227 $C^{\delta1}$ and $C^{\delta2}$, has a LAC at $B = B_{LAC} \approx 1.1$ T, see **Figure 4**. Upon passage through a LAC during the field
228 jump $B_{HF} \rightarrow B_{LF}$ due to the sample shuttle transfer, the population difference is expected to be
229 converted into a coherence between the states, which have the LAC: these adiabatic states correspond
230 to the $|\alpha\alpha\beta\rangle$ and $|\alpha\beta\alpha\rangle$ states at high fields. To calculate the actual spin state at $B = B_{LF}$ we solve
231 numerically the Liouville-von Neumann equation for the spin density operator

$$\frac{d}{dt}\sigma = -i[\hat{\mathcal{H}}(t), \sigma] \tag{9}$$

232 The Hamiltonian of the spin system at a magnetic field B is as follows:

$$\hat{\mathcal{H}}(B) = -\gamma_C B \sum_{i=1}^{3}(1 + \delta_{Ci})\hat{I}_{iz} - \gamma_H B \sum_{j=1}^{7}(1 + \delta_{Hj})\hat{S}_{iz} + 2\pi\sum_{i \neq k} J_{Cik}\left(\hat{\mathbf{I}}_i \cdot \hat{\mathbf{I}}_k\right) \tag{10}$$
$$+ 2\pi\sum_{j \neq m} J_{Hjm}\left(\hat{\mathbf{S}}_j \cdot \hat{\mathbf{S}}_m\right) + 2\pi\sum_{i=1}^{3}\sum_{j=1}^{7} J'_{ij}\hat{I}_{iz}\hat{S}_{jz}$$

233 Here γ_C and γ_H are the carbon and proton gyromagnetic ratios, δ_{Ci} and δ_{Hj} are the chemical shifts of the
234 i-th carbon and j-th proton, J_{Cik} is the scalar coupling constant between the i-th and k-th carbon, J_{Hjm} is
235 the scalar coupling constant between the j-th and m-th proton, J'_{ij} is the scalar coupling constant between
236 the i-th carbon and j-th proton, $\hat{\mathbf{I}}_i$ and $\hat{\mathbf{S}}_j$ are the spin operator of the i-th carbon and j-th proton. Given
237 the range of magnetic fields considered here, heteronuclear scalar couplings are considered to be weak.

238 **Table 1**. Parameters used for energy calculations. Proton-carbon direct scalar coupling values marked by asterisk
239 have been used in numerical simulations of polarization transfer:

Chemical shifts	
C^γ	24.14 ppm
$C^{\delta1}$	22.05 ppm
$C^{\delta2}$	20.92 ppm

Scalar couplings	
J(C^γ- $C^{\delta1}$)	35 Hz
J(C^γ- $C^{\delta2}$)	35.4 Hz
J($C^{\delta1}$- $C^{\delta2}$)	0 Hz
J(C^γ- H^γ)*	127.4 Hz
J($C^{\delta1}$- $H^{\delta1}$)*	124.8 Hz
J($C^{\delta2}$- $H^{\delta2}$)*	124.8 Hz

240 The precise values of the calculation parameters are given in **Table 1**. Since the magnetic field B changes
241 with time, the Hamiltonian $\hat{\mathcal{H}}$ is also time-dependent. In the calculation we consider three carbons and
242 seven protons (six protons in three CH$_3$-groups and the γ-proton). Using this Hamiltonian we evaluate the
243 density operator after the first field jump, $\sigma(t = t_1)$. The Liouville-von Neumann equation is integrated

244 using 1 ms time increments and assuming that for each step the Hamiltonian is constant, similarly to
245 simulations carried out for relaxation experiments (Bolik-Coulon et al., 2020). In the calculation, we ignore
246 relaxation effects, since the dimensionality of the relaxation superoperator is too big for the multi-spin
247 system considered here and our focus is on coherent effects.

248 At $B = B_{LF}$ the density operator evolves under a constant Hamiltonian, at the end of the evolution period
249 it becomes as follows:

$$\sigma(t_1 + \tau) = \exp\left(-i\widehat{\mathcal{H}}(B_{LF})\tau\right)\sigma(t_1)\exp\left(i\widehat{\mathcal{H}}(B_{LF})\tau\right) \tag{11}$$

250 The $B_{LF} \to B_{HF}$ field jump is simulated numerically in the same way as the first field jump (the time
251 interval is split into many small steps). Finally, knowing the density operator σ_{fin} at $t = t_1 + \tau + t_2$, we
252 evaluate the NMR signals of the nuclei of interest as the expectation values of their z-magnetization
253 $\langle I_{iz} \rangle = \text{Tr}\{\hat{I}_{iz}\sigma_{fin}\}$.

254 The method used for modelling the experiments with decoupling at $B = B_{LF}$ is different. After evaluating
255 the density operator $\sigma(t = t_1)$ we trace out the proton degree of freedom and define the density
256 operator of the carbon subsystem as $\sigma_C(t_1) = \text{Tr}_H\{\sigma(t_1)\}$, with the argument that proton polarization is
257 destroyed by decoupling. The partial trace procedure implies that when $\sigma_{ik,jl}$ is a proton-carbon density
258 operator (in the notation of spin states i, j stand for the proton states and k, l stand for the carbon states),
259 the elements of the carbon density operator are: $\{\sigma_C\}_{k,l} = \sum_i \sigma_{ik,il}$. One should note that proton two-
260 spin operators may contain a zero-quantum component, which would stand proton decoupling.
261 Consideration of effects of such coherences is beyond the scope of this work: we expect this to only lead
262 to small perturbations of the observed behavior. Then we introduce the Hamiltonian of the carbon
263 subsystem

$$\widehat{\mathcal{H}}_C(B_{LF}) = -\gamma_C B_{LF} \sum_{i=1}^{3}(1 + \delta_{Ci})\hat{I}_{iz} + 2\pi \sum_{i \neq k} J_{Cik}\left(\hat{\mathbf{I}}_i \cdot \hat{\mathbf{I}}_k\right) \tag{12}$$

264 Using this Hamiltonian, we evaluate the density operator of the ^{13}C spins at the end of the evolution period
265 as follows

$$\sigma_C(t_1 + \tau) = \exp\left(-i\widehat{\mathcal{H}}_C(B_{LF})\tau\right)\sigma_C(t_1)\exp\left(i\widehat{\mathcal{H}}_C(B_{LF})\tau\right) \tag{13}$$

266 The final step in evaluating the ZQC evolution is introducing the carbon-proton density operator. This is
267 done by multiplying $\sigma_C(t_1 + \tau)$ and the density operator of non-polarized protons (as decoupling removes
268 any proton spin order). Hence,

$$\sigma(t_1 + \tau) = \sigma_C(t_1 + \tau) \otimes \sigma_H^{dec}, \quad \sigma_H^{dec} = \frac{1}{2^7}\prod_{j=1}^{7}\hat{1} \tag{14}$$

269 where $\hat{1}$ is a 2×2 unity matrix. The final step of the calculation, the field jump $B_{LF} \to B_{HF}$, is modelled
270 in the same way as in the previous case.

271 Finally, we would like to comment on the $B(t)$ dependence, which was used in calculation. The distance
272 dependence of the magnetic field $B(z)$ is precisely known but the precise $z(t)$ is not known. We modelled
273 this dependence assuming that motion goes with a constant speed (in experiments, constant-speed
274 motion is achieved after a 5-10 ms lag delay for acceleration). Non-ideal agreement between theory and
275 experiment can be attributed to the fact that the precise $z(t)$ dependence is not known (our previous
276 works (Pravdivtsev et al., 2013; Kiryutin et al., 2013) show that the knowledge of $z(t)$ is required for
277 modeling).
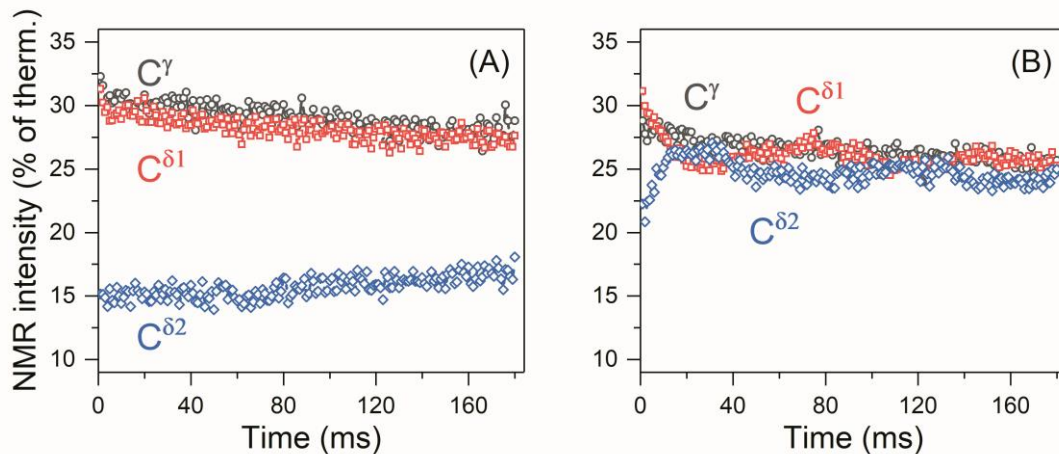
Figure 5. Observed τ-dependence of the polarizations of carbon-13 nuclei C$^\gamma$, C$^{\delta1}$ and C$^{\delta2}$ measured (A) without ^{1}H decoupling, and (B) with ^{1}H decoupling. The NMR intensities are plotted in percent of the intensities of the NMR signals in the 150.9 MHz ^{13}C spectra (i.e., at 14.1 T) at thermal equilibrium.

IV. Results and discussion

The experimental τ-dependences of the measured spin polarization are shown in **Figure 5**. One can see that without decoupling no coherent behavior is found: polarization simply decays due to relaxation and no coherent oscillations are visible (**Figure 5A**). In the presence of proton decoupling (**Figure 5B**) the situation is drastically different: coherent oscillations are clearly observed, which mediate polarization exchange between the C$^{\delta1}$ and C$^{\delta2}$ nuclei. We attribute such polarization exchange to the ZQC, which is generated by passage through the LAC. The coherence gives rise to exchange of the populations of the two states, which experience the LAC. These levels are correlated with the $|\alpha\alpha\beta\rangle$ and $|\alpha\beta\alpha\rangle$ high-field states. Hence, polarization transfer gives rise to population exchange of the states $|\alpha\alpha\beta\rangle$ (initially overpopulated state) and $|\alpha\beta\alpha\rangle$ (initially underpopulated state). As a result, the state of the first spin, C$^\gamma$, does not change, but the other two spins, C$^{\delta1}$ and C$^{\delta2}$, exchange polarizations. With the available speed and range of the field-cycling, other coherences are not excited, i.e., non-adiabatic variation of the Hamiltonian is achieved only for the pairs of levels that have the LAC in between B_{LF} and B_{HF}, i.e., only the LAC shown in **Figure 4** contributes to spin mixing. The C$^\gamma$ spin never shows any oscillatory polarization transfer, which is an indication that the specific LAC is responsible for the observed effect. In conclusion, a zero-quantum coherence of the two carbon-13 nuclei C$^{\delta1}$ and C$^{\delta2}$ is excited by fast magnetic field jump between 14.1 T and 0.33 T.

Hence, the oscillatory behavior does not show up in the absence of proton decoupling. There are two reasons for that. First, the multiple proton-carbon couplings give rise to a set of ZQC frequencies, instead of a unique frequency in the presence of decoupling. Second and more importantly, proton-carbon-13 couplings prevent the carbon subsystem from reaching the strong-coupling regime. Thus, the amplitude of coherent evolutions is drastically reduced (see Eq. 7) and becomes negligible (**Figure 5A**). As a result, in experiments without decoupling the ZQC decays because of inhomogeneous broadening of the ZQC evolution frequency, *i.e.* relaxation. We would like to stress that the ZQC of interest is excited by the field jump, which is identical for experiments with and without proton decoupling at low field. However, the ZQC does not reveal itself and does not give rise to efficient polarization transfer in the experiment without decoupling.

These considerations are confirmed by theoretical modeling (**Figure 6**). In the presence of carbon-proton couplings coherent oscillations are hardly observed: only fast oscillations of very small amplitude can be seen in the simulated curves. By contrast, in the absence of the proton-carbon couplings, i.e., when decoupling is used, coherent evolutions become manifest with slower oscillations of larger amplitude. The results of numerical modeling are in good agreement with the experimental data. As relaxation effects

314 are not taken into account in simulations, to ease comparison we subtracted the slowly relaxing
315 background from the experimental time traces. In addition, we rescaled all calculated traces with the
316 same factor; then the starting polarization values were adjusted individually to achieve the best
317 agreement with the experimental data. Such a data treatment becomes necessary because relaxation is
318 active not only during spin mixing at the B_{LF} field, but also during the field jumps. The agreement between
319 the experimental data and simulation in **Figure 6** is not ideal, possibly because some small long-range
320 scalar couplings are not included in the simulation but most likely because the field switching profile is
321 not known exactly: previous studies of the spin dynamics in field-cycling NMR experiments (Pravdivtsev
322 et al., 2013; Kiryutin et al., 2013) suggest that using the precise $B(t)$ profile is crucial for simulating
323 coherent polarization transfer phenomena.
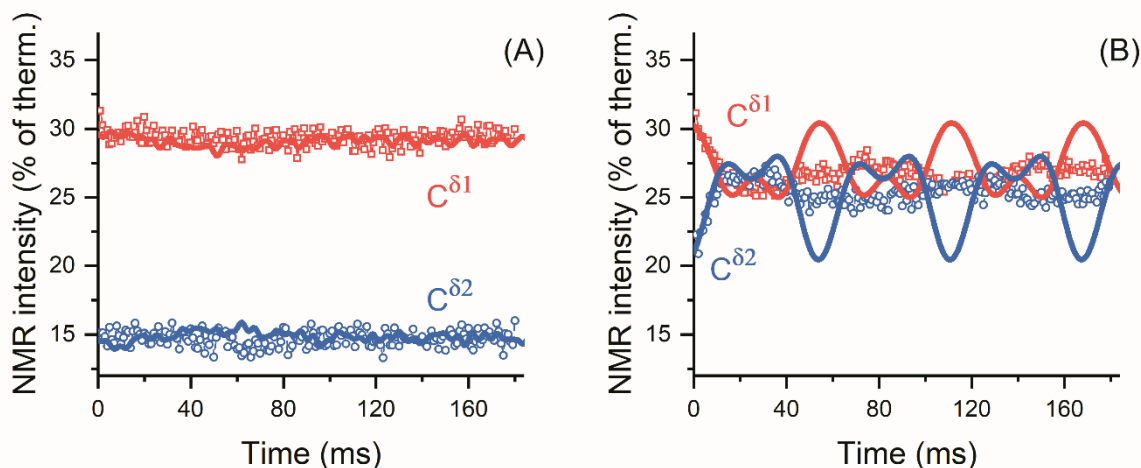
324
325 **Figure 6**. Calculated τ-dependence of polarization (lines) overlaid with the observed time traces (points) obtained
326 (A) without ^{1}H decoupling, and (B) with ^{1}H decoupling. The slowly relaxing background (compare with the data shown
327 in **Figure 5**) has been subtracted from the time traces, to enable comparison between theory and simulations.
328 Observed NMR intensities are normalized to intensities in 150.9 MHz (14.1 T) ^{13}C spectra at thermal equilibrium. We
329 use the subtraction procedure because relaxation effects were not taken into account in the calculation;
330 consequently, we are unable to consider polarization decay due to relaxation at B_{LF} and during the field variation.
331 To enable comparison of the experiment and calculation results, the amplitude of oscillations in polarization transfer
332 traces were scaled with the same factor, then the starting polarization values were adjusted individually to give best
333 agreement with experimental data.

334 The absence of strong-coupling regime, in spite of scalar coupling constants larger than the difference in
335 Larmor frequencies is somewhat counterintuitive but clearly explained when taking into account the
336 effect of large heteronuclear scalar couplings (Eqs. 2-4). In the present case, the effect is even more
337 pronounced, since the two δ carbon-13 nuclei of leucine are coupled to no less than 3 protons each,
338 further splitting resonance frequencies in the absence of proton decoupling. A conventional way to
339 present the weak coupling regime consists in stating that the part of the scalar coupling Hamiltonian (Eq.
340 1) that is proportional to a zero-quantum product operator is non-secular in the frame of the Zeeman
341 interactions of the two coupled spins, which is true if the scalar coupling constant is much smaller than
342 the difference in Larmor frequencies of the two spins. Here, the weak-coupling regime is extended
343 because this zero-quantum part can be considered non-secular in the interaction frame of the
344 heteronuclear scalar couplings (note that the perturbative treatment is allowed to the extent that the
345 heteronuclear coupling constants are much larger than the homonuclear coupling).

346 A particular consequence of the observation we report here can be relevant for experiments where the
347 strong scalar-coupling regime is created by radio-frequency irradiation: isotropic mixing for TOCSY
348 (Braunschweiler and Ernst, 1983). We have recently introduced a two-field TOCSY experiment where
349 isotropic mixing is carried out at 0.33 T and chemical shift evolutions occur at high field (Kadeřávek et al.,
350 2017), which makes broadband carbon-13 TOCSY straightforward. This study included a control

experiment where no radio-frequency pulses were applied at low field (see Figure 3.b in reference (Kadeřávek et al., 2017). Intuitively, one would have expected cross-peaks to be observed for carbon-13 nuclei in strongly-coupled networks at 0.33 T. Some cross peaks could indeed be observed within the aliphatic carbon region of leucine and in the aromatic ring of phenylalanine. The current investigation suggests that strong scalar couplings between carbon-13 nuclei are less prevalent than expected at 0.33 T. The observed cross-peaks were possibly due to cross-relaxation and not necessarily coherent evolution under strong scalar couplings. Conventional TOCSY experiments might also be altered by the effect of large heteronuclear scalar couplings. In this case, isotropic mixing sequences have been optimized on isolated pairs of two coupled spins (Kadkhodaie et al., 1991), excluding the effects of scalar couplings to heteronuclei or as heteronuclear decoupling sequences that happen to be efficient at isotropic mixing (Rucker and Shaka, 1989; Shaka et al., 1988). Although isotropic mixing sequences decouple heteronuclear scalar couplings, optimizing simultaneously for homo- and heteronuclear scalar coupling operators may improve homonuclear coherence transfers. Such effects of couplings to heteronuclei are of relevance for abundant nuclei (protons), whereas for other nuclei they become important when uniform spin labelling is used.

V. Conclusions

In this work, we present a study of coherent polarization transfer in a system of (strongly) coupled ^{13}C nuclei. Spin coherences are zero-quantum coherences, which are generated by a fast non-adiabatic magnetic field jump. Such coherences are excited most efficiently when the system goes through a LAC during the field switch. Here we indeed pass through a LAC in a system of three coupled ^{13}C spins and investigate the spin dynamics at low fields, where strong couplings of the carbon spins are expected.

We can clearly demonstrate that the polarization transfer in the carbon-13 spin subsystem is strongly affected by spin-spin interactions with the protons in the molecule. In this situation, the role of these interactions can be determined by comparing the experiments with and without proton decoupling at low fields. When decoupling is used, we observe coherent polarization exchange between two of the three carbons: such a behavior is typical when the spin coherences are excited upon non-adiabatic passage through a specific LAC. In the absence of decoupling, i.e., when heteronuclear interactions are present, we cannot observe such a behavior: polarization transfer is very inefficient and coherent phenomena are not found. We attribute this to the fact that relatively strong proton-carbon couplings (i) drive the carbon system away from the strong coupling condition and (ii) give rise to a set of evolution frequencies instead of a unique ZQC frequency. These considerations are supported by an analytical model of a three-spin system and numerical simulations in a multi-spin system.

Our results are of importance for analyzing polarization transfer phenomena at low magnetic fields and for interpreting NMR data obtained under apparent strong coupling conditions. Under such conditions heteronuclear spin-spin interactions might disturb "strong coupling" of homonuclei and substantially alter spin dynamics. Similar effects also often arise in dynamic nuclear polarization, where the difference in the electron-nuclear couplings for nuclei located at different distances from the electron hampers nuclear spin diffusion, giving rise to the spin diffusion barrier around the electron spin (Ramanathan, 2008).

Acknowledgements

This work has been supported by the Russian Foundation for Basic Research (grants Nos. 19-29-10028 and 19-33-90251). I.V.Z. acknowledges support from the French embassy in the Russian Federation, in the framework of the Ostrogradsky fellowship (project No. 933824A).

References

Appelt, S., Häsing, F. W., Sieling, U., Gordji-Nejad, A., Glöggler, S., and Blümich, B.: Paths from Weak to Strong Coupling in NMR, Phys. Rev. A, 81, 023420, https://doi.org/10.1103/PhysRevA.81.023420, 2010.

396 Blanchard, J. W., and Budker, D.: Zero- to Ultralow-Field NMR, eMagRes, 5, 1395-1409,
397 https://doi.org/10.1002/9780470034590.emrstm1369, 2016.

398 Bodenhausen, G., Freeman, R., Morris, G. A., and Turner, D. L.: Proton-Coupled Carbon-13 J Spectra in the
399 Presence of Strong Coupling. II, J. Magn. Reson., 28, 17-28, https://doi.org/10.1016/0022-2364(77)90252-
400 9, 1977.

401 Bolik-Coulon, N., Kaderavek, P., Pelupessy, P., Dumez, J. N., Ferrage, F., and Cousin, S. F.: Theoretical and
402 Computational Framework for the Analysis of the Relaxation Properties of Arbitrary Spin Systems.
403 Application to High-Resolution Relaxometry, J. Magn. Reson., 313,
404 https://doi.org/10.1016/j.jmr.2020.106718, 2020.

405 Braunschweiler, L., and Ernst, R. R.: Coherence Transfer by Isotropic Mixing - Application to Proton
406 Correlation Spectroscopy, J. Magn. Reson., 53, 521-528, https://doi.org/10.1016/0022-2364(83)90226-3,
407 1983.

408 Bryant, R. G., and Korb, J. P.: Nuclear Magnetic Resonance and Spin Relaxation in Biological Systems,
409 Magn. Reson. Imaging, 23, 167-173, https://doi.org/10.1016/j.mri.2004.11.026, 2005.

410 Cavanagh, J.: Protein NMR Spectroscopy : Principles and Practice, 2nd ed., Academic Press, Amsterdam ;
411 Boston, xxv, 885 p. pp., 2007.

412 Charlier, C., Khan, S. N., Marquardsen, T., Pelupessy, P., Reiss, V., Sakellariou, D., Bodenhausen, G.,
413 Engelke, F., and Ferrage, F.: Nanosecond Time Scale Motions in Proteins Revealed by High-Resolution NMR
414 Relaxometry, J. Am. Chem. Soc., 135, 18665-18672, https://doi.org/10.1021/ja409820g, 2013.

415 Chou, C.-Y., Chu, M., Chang, C.-F., Yu, T., Huang, T.-h., and Sakellariou, D.: High Sensitivity High-Resolution
416 Full Range Relaxometry Using a Fast Mechanical Sample Shuttling Device and a Cryo-Probe, J. Biomol.
417 NMR, 66, 187-194, https://doi.org/10.1007/s10858-016-0066-5, 2016.

418 Chou, C.-Y., Abdesselem, M., Bouzigues, C., Chu, M., Guiga, A., Huang, T.-H., Ferrage, F., Gacoin, T.,
419 Alexandrou, A., and Sakellariou, D.: Ultra-Wide Range Field-Dependent Measurements of the Relaxivity
420 of $Gd_{1-x}Eu_xVO_4$ Nanoparticle Contrast Agents Using a Mechanical Sample-Shuttling Relaxometer, Sci. Rep.,
421 7, 44770, https://doi.org/10.1038/srep44770, 2017.

422 Cousin, S. F., Charlier, C., Kaderavek, P., Marquardsen, T., Tyburn, J. M., Bovier, P. A., Ulzega, S., Speck, T.,
423 Wilhelm, D., Engelke, F., Maas, W., Sakellariou, D., Bodenhausen, G., Pelupessy, P., and Ferrage, F.: High-
424 Resolution Two-Field Nuclear Magnetic Resonance Spectroscopy, Phys. Chem. Chem. Phys., 18, 33187-
425 33194, https://doi.org/10.1039/c6cp05422f, 2016a.

426 Cousin, S. F., Kaderavek, P., Haddou, B., Charlier, C., Marquardsen, T., Tyburn, J. M., Bovier, P. A., Engelke,
427 F., Maas, W., Bodenhausen, G., Pelupessy, P., and Ferrage, F.: Recovering Invisible Signals by Two-Field
428 NMR Spectroscopy, Angew. Chem., Int. Ed., 55, 9886-9889, https://doi.org/10.1002/anie.201602978,
429 2016b.

430 Ernst, R. R., Bodenhausen, G., and Wokaun, A.: Principles of Nuclear Magnetic Resonance in One and Two
431 Dimensions, The International Series of Monographs on Chemistry, 14, Clarendon Press; Oxford University
432 Press, Oxford Oxfordshire, New York, 1987.

433 Foroozandeh, M., Adams, R. W., Meharry, N. J., Jeannerat, D., Nilsson, M., and Morris, G. A.: Ultrahigh-
434 Resolution NMR Spectroscopy, Angew. Chem., Int. Ed., 53, 6990-6992,
435 https://doi.org/10.1002/anie.201404111, 2014.

436 Geen, H., and Freeman, R.: Band-Selective Radiofrequency Pulses, J. Magn. Reson., 93, 93-141,
437 https://doi.org/10.1016/0022-2364(91)90034-Q, 1991.

438 Goddard, Y., Korb, J.-P., and Bryant, R. G.: The Magnetic Field and Temperature Dependences of Proton
439 Spin-Lattice Relaxation in Proteins, J. Chem. Phys., 126, 175105, https://doi.org/10.1063/1.2727464,
440 2007.

441 Grootveld, M., Percival, B., Gibson, M., Osman, Y., Edgar, M., Molinari, M., Mather, M. L., Casanova, F.,
442 and Wilson, P. B.: Progress in Low-Field Benchtop NMR Spectroscopy in Chemical and Biochemical
443 Analysis, Anal. Chim. Acta, 1067, 11-30, https://doi.org/10.1016/j.aca.2019.02.026, 2019.

444 Ivanov, K. L., Miesel, K., Yurkovskaya, A. V., Korchak, S. E., Kiryutin, A. S., and Vieth, H.-M.: Transfer of
445 CIDNP among Coupled Spins at Low Magnetic Field, Appl. Magn. Reson., 30, 513-534,
446 https://doi.org/10.1007/Bf03166215, 2006.

447 Ivanov, K. L., Yurkovskaya, A. V., and Vieth, H.-M.: Coherent Transfer of Hyperpolarization in Coupled Spin
448 Systems at Variable Magnetic Field, J. Chem. Phys., 128, 154701, https://doi.org/10.1063/1.2901019,
449 2008.

Ivanov, K. L., Pravdivtsev, A. N., Yurkovskaya, A. V., Vieth, H.-M., and Kaptein, R.: The Role of Level Anti-Crossings in Nuclear Spin Hyperpolarization, Prog. Nucl. Magn. Reson. Spectrosc., 81, 1-36, https://doi.org/10.1016/j.pnmrs.2014.06.001, 2014.

Kadeřávek, P., Strouk, L., Cousin, S. F., Charlier, C., Bodenhausen, G., Marquardsen, T., Tyburn, J. M., Bovier, P. A., Engelke, F., Maas, W., and Ferrage, F.: Full Correlations across Broad NMR Spectra by Two-Field Total Correlation Spectroscopy, ChemPhysChem, 18, 2772-2776, https://doi.org/10.1002/cphc.201700369, 2017.

Kadkhodaie, M., Rivas, O., Tan, M., Mohebbi, A., and Shaka, A. J.: Broad-Band Homonuclear Cross Polarization Using Flip-Flop Spectroscopy, J. Magn. Reson., 91, 437-443, https://doi.org/10.1016/0022-2364(91)90210-K, 1991.

Keeler, J.: Understanding NMR Spectroscopy, Wiley, Chichester, England; Hoboken, NJ, xv, 459 p. pp., 2005.

Kiryutin, A. S., Yurkovskaya, A. V., Kaptein, R., Vieth, H.-M., and Ivanov, K. L.: Evidence for Coherent Transfer of Para-Hydrogen-Induced Polarization at Low Magnetic Fields, J. Phys. Chem. Lett., 4, 2514-2519, https://doi.org/10.1021/jz401210m, 2013.

Kiryutin, A. S., Pravdivtsev, A. N., Ivanov, K. L., Grishin, Y. A., Vieth, H.-M., and Yurkovskaya, A. V.: A Fast Field-Cycling Device for High-Resolution NMR: Design and Application to Spin Relaxation and Hyperpolarization Experiments, J. Magn. Reson., 263, 79-91, https://doi.org/10.1016/j.jmr.2015.11.017, 2016.

Korchak, S. E., Ivanov, K. L., Pravdivtsev, A. N., Yurkovskaya, A. V., Kaptein, R., and Vieth, H.-M.: High Resolution NMR Study of T_1 Magnetic Relaxation Dispersion. III. Influence of Spin 1/2 Hetero-Nuclei on Spin Relaxation and Polarization Transfer among Strongly Coupled Protons, J. Chem. Phys., 137, 094503, https://doi.org/10.1063/1.4746780, 2012.

Ledbetter, M. P., Theis, T., Blanchard, J. W., Ring, H., Ganssle, P., Appelt, S., Blümich, B., Pines, A., and Budker, D.: Near-Zero-Field Nuclear Magnetic Resonance, Phys. Rev. Lett., 107, 107601, https://doi.org/10.1103/PhysRevLett.107.107601, 2011.

Levitt, M. H., Freeman, R., and Frenkiel, T.: Supercycles for Broad-Band Heteronuclear Decoupling, J. Magn. Reson., 50, 157-160, https://doi.org/10.1016/0022-2364(82)90042-7, 1982.

Levitt, M. H.: Spin Dynamics : Basics of Nuclear Magnetic Resonance-2nd Ed., 2008.

Miesel, K., Ivanov, K. L., Yurkovskaya, A. V., and Vieth, H.-M.: Coherence Transfer During Field-Cycling NMR Experiments, Chem. Phys. Lett., 425, 71-76, https://doi.org/10.1016/j.cplett.2006.05.025, 2006.

Pfändler, P., and Bodenhausen, G.: Strong Coupling Effects in Z-Filtered Two-Dimensional NMR Correlation Spectra, J. Magn. Reson., 72, 475-492, https://doi.org/10.1016/0022-2364(87)90152-1, 1987.

Pravdivtsev, A. N., Yurkovskaya, A. V., Kaptein, R., Miesel, K., Vieth, H.-M., and Ivanov, K. L.: Exploiting Level Anti-Crossings for Efficient and Selective Transfer of Hyperpolarization in Coupled Nuclear Spin Systems, Phys. Chem. Chem. Phys., 15, 14660-14669, https://doi.org/10.1039/c3cp52026a, 2013.

Ramanathan, C.: Dynamic Nuclear Polarization and Spin Diffusion in Nonconducting Solids, Appl. Magn. Reson., 34, 409-421, 2008.

Redfield, A. G.: High-Resolution NMR Field-Cycling Device for Full-Range Relaxation and Structural Studies of Biopolymers on a Shared Commercial Instrument, J. Biomol. NMR, 52, 159-177, https://doi.org/10.1007/s10858-011-9594-1, 2012.

Roberts, M. F., and Redfield, A. G.: Phospholipid Bilayer Surface Configuration Probed Quantitatively by ^{31}P Field-Cycling NMR, Proc. Natl. Acad. Sci. U. S. A., 101, 17066-17071, https://doi.org/10.1007/s10858-011-9594-1, 2004a.

Roberts, M. F., and Redfield, A. G.: High-Resolution ^{31}P Field Cycling NMR as a Probe of Phospholipid Dynamics, J. Am. Chem. Soc., 126, 13765-13777, https://doi.org/10.1021/ja046658k, 2004b.

Rucker, S. P., and Shaka, A. J.: Broad-Band Homonuclear Cross Polarization in 2D NMR Using DIPSI-2, Mol. Phys., 68, 509-517, https://doi.org/10.1080/00268978900102331, 1989.

Shaka, A. J., Keeler, J., Frenkiel, T., and Freeman, R.: An Improved Sequence for Broad-Band Decoupling - WALTZ-16, J. Magn. Reson., 52, 335-338, https://doi.org/10.1016/0022-2364(83)90207-X, 1983.

Shaka, A. J., Lee, C. J., and Pines, A.: Iterative Schemes for Bilinear Operators - Application to Spin Decoupling, J. Magn. Reson., 77, 274-293, https://doi.org/10.1016/0022-2364(88)90178-3, 1988.

502 Tayler, M. C. D., Theis, T., Sjolander, T. F., Blanchard, J. W., Kentner, A., Pustelny, S., Pines, A., and Budker,
503 D.: Invited Review Article: Instrumentation for Nuclear Magnetic Resonance in Zero and Ultralow
504 Magnetic Field, Rev. Sci. Instrum., 88, 091101, https://doi.org/10.1063/1.5003347, 2017.
505 Türschmann, P., Colell, J., Theis, T., Blümich, B., and Appelt, S.: Analysis of Parahydrogen Polarized Spin
506 System in Low Magnetic Fields, Phys. Chem. Chem. Phys., 16, 15411-15421,
507 https://doi.org/10.1039/c4cp01807a, 2014.
508 Vallurupalli, P., Scott, L., Williamson, J. R., and Kay, L. E.: Strong Coupling Effects During X-Pulse CPMG
509 Experiments Recorded on Heteronuclear ABX Spin Systems: Artifacts and a Simple Solution, J. Biomol.
510 NMR, 38, 41-46, https://doi.org/10.1007/s10858-006-9139-1, 2007.
511 Wagner, S., Dinesen, T. R. J., Rayner, T., and Bryant, R. G.: High-Resolution Magnetic Relaxation Dispersion
512 Measurements of Solute Spin Probes Using a Dual-Magnet System, J. Magn. Reson., 140, 172-178,
513 https://doi.org/10.1006/jmre.1999.1811, 1999.
514 Zhukov, I. V., Kiryutin, A. S., Yurkovskaya, A. V., Grishin, Y. A., Vieth, H.-M., and Ivanov, K. L.: Field-Cycling
515 NMR Experiments in Ultra-Wide Magnetic Field Range: Relaxation and Coherent Polarization Transfer,
516 Phys. Chem. Chem. Phys., 20, 12396-12405, https://doi.org/10.1039/C7CP08529J, 2018.